

On the Reactions of $[\text{RuCl}_2(\text{PPh}_3)_3]$ with Thia Crown Ethers: Molecular Structures of $[\text{RuCl}_2(\text{PPh}_3)([9]\text{aneS}_3)]$ ($[9]\text{aneS}_3 = 1,4,7\text{-trithiacyclononane}$) and $[\text{RuCl}(\text{PPh}_3)([14]\text{aneS}_4)]\text{ClO}_4$ ($[14]\text{aneS}_4 = 1,4,8,11\text{-tetrathiacyclotetradecane}$)†

Nathaniel W. Alcock,^a Jason C. Cannadine,^a George R. Clark^b and Anthony F. Hill^{*,c}

^a Department of Chemistry, University of Warwick, Coventry CV4 7AL, UK

^b Department of Chemistry, University of Auckland, Auckland, New Zealand

^c Department of Chemistry, Imperial College of Science, Technology and Medicine, South Kensington, London SW7 2AY, UK

The reaction of $[\text{RuCl}_2(\text{PPh}_3)_3]$ with 1,4,7-trithiacyclononane ($[9]\text{aneS}_3$) gives the neutral complex $[\text{RuCl}_2(\text{PPh}_3)([9]\text{aneS}_3)]$ while the same complex with 1,4,8,11-tetrathiacyclotetradecane ($[14]\text{aneS}_4$) followed by chloride-perchlorate metathesis provides the salt *cis*- $[\text{RuCl}(\text{PPh}_3)([14]\text{aneS}_4)]\text{ClO}_4$. The structures of both complexes have been determined by X-ray crystallography.

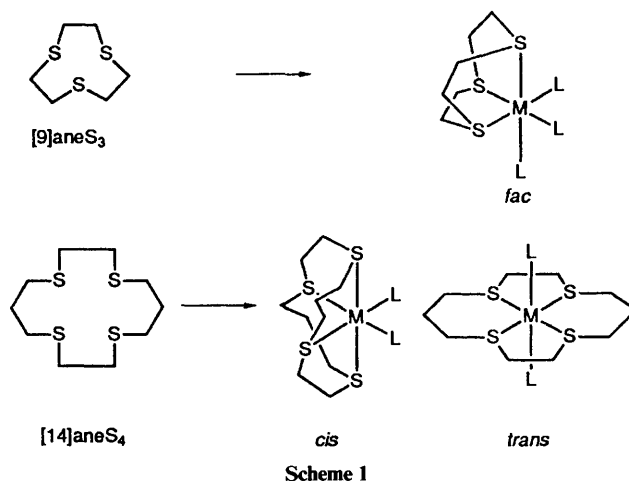
The bulk of co-ordination chemistry investigated to date for thia crown ethers involves the simple 1:1 or 2:1 adducts with metal halides.^{1,2} Thus, for example, the sulfur macrocycle 1,4,7-trithiacyclononane ($[9]\text{aneS}_3$, Scheme 1) has been shown to bind to a large number of metal centres in a variety of oxidation states; however very little is known about the chemical properties which such co-ordination confers upon the metal co-ordination sphere. This is despite the claim¹ that these ligands may enjoy application as co-ligands in the design of robust organometallic catalysts.

A rare, but inspiring indication that thia crown ethers are compatible with organometallic ligand systems is provided by the recent work of Schröder and co-workers³ dealing with the co-ordination of $[9]\text{aneS}_3$ to low-valent rhodium centres wherein it was shown that a range of typical organometallic ligands (olefins, σ -alkyls) could be supported by this ligand. We have also shown recently^{4,5} that σ -vinyl, thiocarbonyl and thioacyl ligands are also compatible with the $[9]\text{aneS}_3$ ligand, by drawing upon the notional similarity between the co-ordinating properties of $[9]\text{aneS}_3$, hydrotris(pyrazol-1-yl)-borate, arene and cyclopentadienyl ligands (Scheme 2).

As part of a programme to investigate the organometallic chemistry of sulfur macrocycles we have investigated the reactions of $[\text{RuCl}_2(\text{PPh}_3)_3]$ with $[9]\text{aneS}_3$ and 1,4,8,11-tetrathiacyclotetradecane ($[14]\text{aneS}_4$) and find that the former provides a neutral complex $[\text{RuCl}_2(\text{PPh}_3)([9]\text{aneS}_3)]$ whilst the latter provides salts of the cationic complex *cis*- $[\text{RuCl}(\text{PPh}_3)([14]\text{aneS}_4)]^+$. Aspects of this work have provided the basis of a preliminary report.⁵

Experimental

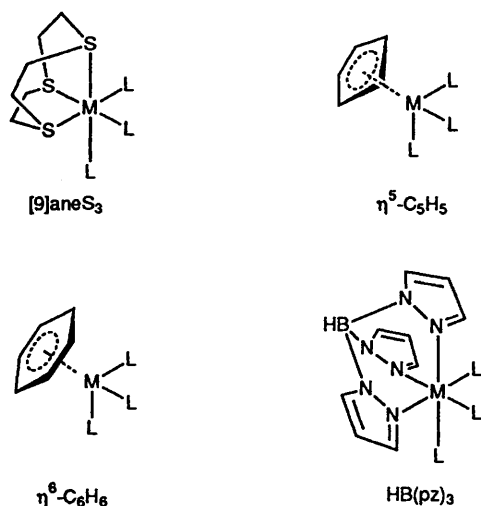
General Procedures.—All manipulations were carried out under an atmosphere of pre-purified dinitrogen using conventional Schlenk-tube techniques. Solvents were purified by distillation from an appropriate drying agent (ethers and alkanes from sodium-potassium alloy with benzophenone as indicator; halogenocarbons from CaH_2 and alcohols from the corresponding alkoxide).



Proton and $^{31}\text{P}\{-^1\text{H}\}$ NMR spectra were recorded on a Bruker WH-400 or Perkin Elmer R34 NMR spectrometer and calibrated against internal SiMe_4 (^1H) or external H_3PO_4 (^{31}P). Infrared spectra were recorded using a Perkin Elmer 1720-X Fourier-transform IR spectrometer and FAB mass spectrometry carried out using a Kratos MS80 mass spectrometer employing 3-nitrobenzyl alcohol as the matrix. The complex $[\text{RuCl}_2(\text{PPh}_3)_3]$ ⁶ has been described elsewhere. 1,4,7-Tri-thiacyclononane ($[9]\text{aneS}_3$) and 1,4,8,11-tetrathiacyclotetradecane ($[14]\text{aneS}_4$) were obtained commercially (Aldrich) and used as received.

Synthesis of $[\text{RuCl}_2(\text{PPh}_3)([9]\text{aneS}_3)]$.—A dark red solution of $[9]\text{aneS}_3$ (0.100 g, 0.5 mmol) and $[\text{RuCl}_2(\text{PPh}_3)_3]$ (0.531 g, 0.55 mmol) in dichloromethane (20 cm^3 , degassed) was stirred for 90 min under an atmosphere of nitrogen. Addition of ethanol (50 cm^3) followed by concentration (rotary evaporator) of the solution to ca. 15 cm^3 provided yellow crystals of the desired product. Yield 0.234 g (70%) as a dichloromethane monosolvate (^1H NMR) (Found: C, 42.0; H, 4.4. $\text{C}_{24}\text{H}_{27}\text{Cl}_2\text{PRuS}_3\cdot\text{CH}_2\text{Cl}_2$ requires C, 42.9; H, 4.2%). IR (Nujol) 270, 250 cm^{-1} [$\nu(\text{RuCl}_2)$]. NMR (CDCl_3 , 25 °C): ^1H , δ 1.80, 2.15, 2.42, 3.10 (m \times 4, 12 H, $[9]\text{aneS}_3$) 7.30–7.65 (m \times 6, 15 H, PPh_3); ^{31}P , δ 35.0. FAB MS:

† Supplementary data available: see Instructions for Authors, *J. Chem. Soc., Dalton Trans.*, 1993, Issue 1, pp. xxiii–xxviii.



Scheme 2 Six-electron *fac* ligands; pz = pyrazol-1-yl

Table 1 Selected bond lengths (Å) and angles (°) for [RuCl₂(PPh₃)₃]-([9]aneS₃)-CDCl₃ with estimated standard deviations (e.s.d.s) in parentheses

Ru-Cl(1)	2.456(2)	Ru-P	2.345(2)
Ru-Cl(2)	2.449(2)	Ru-S(1)	2.356(2)
Ru-S(2)	2.270(2)	Ru-S(3)	2.269(2)
P-Ru-Cl(1)	94.2(1)	P-Ru-Cl(2)	90.3(1)
Cl(1)-Ru-Cl(2)	95.7(1)	P-Ru-S(2)	96.0(1)
Cl(1)-Ru-S(1)	84.0(1)	Cl(2)-Ru-S(1)	86.0(1)
Cl(1)-Ru-S(2)	88.8(1)	S(1)-Ru-S(2)	87.9(1)
P-Ru-S(3)	93.7(1)	Cl(2)-Ru-S(3)	85.4(1)
S(1)-Ru-S(3)	88.2(1)	S(2)-Ru-S(3)	89.2(1)

m/z 613 (41) [M^+], 395 (13%) [$M - [9]aneS_3 - Cl$]⁺, 307 (100) [$M - [9]aneS_3 - PPh_3$]⁺, 262 (52) PPh₃⁺.

Synthesis of [RuCl(PPh₃)₃][14]aneS₄]AsF₆.—A suspension of [RuCl₂(PPh₃)₃] (0.356 g, 0.37 mmol) and [14]aneS₄ (0.100 g, 0.37 mmol) in degassed dichloromethane (20 cm³) was stirred under an atmosphere of nitrogen for 1 h. Addition of a mixture of NaAsF₆ (100 mg) in water (1.0 cm³) and ethanol (20 cm³) to the resulting solution yielded a yellow-brown precipitate. The suspension was concentrated to ca. 10 cm³, filtered and ethanol (20 cm³) was added to the filtrate to give the desired product, which was isolated by filtration, and washed with ethanol (20 cm³) and diethyl ether (20 cm³). Yield 0.21 g (86%) as an ethanol monosolvate (¹H NMR) (Found: C, 39.3; H, 4.2. C₂₅H₃₅AsClF₆RuS₄·C₂H₅OH requires C, 38.8; H, 4.9%). IR (Nujol) 275 cm⁻¹ [ν(RuCl)]. NMR (CDCl₃, 25 °C): ¹H, δ 2.30, 2.40, 2.75, 2.80, 3.02, 3.10, 3.21, 3.75 (m × 8, 20 H, [14]aneS₄), 7.25–7.58 (m × 5, 15 H, PPh₃); ³¹P, δ 33.0. FAB MS m/z 667 (19) [M^+], 407 (9) [$M - [14]aneS_4$]⁺, 307 (12) [$M - [14]aneS_4 - Ru$]⁺, 262 (100%), PPh₃⁺.

The perchlorate salt, with similar spectroscopic data, was obtained in a completely analogous manner by employing LiClO₄ in place of NaAsF₆ and provided crystals more suitable for X-ray diffractometry.

Structure Determination of [RuCl₂(PPh₃)₃][9]aneS₃]-CDCl₃.—Yellow prisms were grown fortuitously by slow concentration of a solution of the crude material in deuteriochloroform. That chosen for data collection (ca. 0.17 × 0.31 × 0.12 mm) was mounted on a glass fibre. Diffracted intensities were collected (ω–2θ scans) at 298 K on a Nicolet P3m four-circle diffractometer. Of 5755 unique reflections, 3577 had $F \geq 4\sigma(F)$,

Table 2 Atomic coordinates for [RuCl₂(PPh₃)₃][9]aneS₃]-CDCl₃ with e.s.d.s in parentheses

Atom	x	y	z
Ru	3612.6(4)	1117.4(3)	1726.9(2)
P	1630.3(12)	1756.6(9)	1901.9(7)
Cl(1)	4770.5(14)	2444.9(9)	2214.0(9)
Cl(2)	3519.1(14)	1661.7(11)	504.0(7)
S(1)	5627.9(13)	563.1(10)	1488.4(8)
S(2)	3826.9(13)	434.5(9)	2801.0(7)
S(3)	2806.7(13)	-206.9(9)	1274.2(7)
C(1)	5348(6)	-606(4)	1172(3)
C(2)	4097(6)	-671(5)	785(3)
C(3)	2821(6)	-1037(4)	1999(3)
C(4)	2835(5)	-582(4)	2714(3)
C(5)	5395(5)	-95(4)	2852(3)
C(6)	6289(5)	358(4)	2368(3)
C(11)	381(4)	358(4)	1517(3)
C(12)	-54(5)	1037(3)	1875(3)
C(13)	-852(6)	-346(5)	1529(4)
C(14)	-1265(6)	-215(5)	850(5)
C(15)	-876(6)	550(6)	493(4)
C(16)	-40(5)	1163(4)	818(3)
C(21)	1138(5)	1924(3)	2809(3)
C(22)	-114(6)	1890(4)	2979(3)
C(23)	-439(8)	2008(5)	3667(4)
C(24)	447(9)	2172(5)	4194(4)
C(25)	1684(9)	2228(5)	4033(3)
C(26)	2058(6)	2116(4)	3338(3)
C(31)	1279(5)	2888(3)	1509(3)
C(32)	61(6)	3206(4)	1439(3)
C(33)	-189(7)	4048(5)	1123(3)
C(34)	758(7)	4581(4)	886(3)
C(35)	1988(6)	4266(4)	960(4)
C(36)	2246(6)	3426(4)	1267(3)
C(001)	4102(6)	8171(5)	4862(3)
Cl(01)	3978.6(25)	9281.0(16)	4512.3(12)
Cl(02)	2714.8(19)	7578.1(15)	4698.8(13)
Cl(03)	4498.9(23)	8222.8(15)	5763.7(11)

and only these data were used in the solution and refinement of the structure. Corrections were applied for Lorentz, polarization and X-ray absorption effects, the latter by an analytical method based on complete definition of crystal morphology.

Crystal data. C₂₅H₂₇Cl₅DPS₃Ru, $M = 758.04$, monoclinic, $a = 10.652(4)$, $b = 14.598(7)$, $c = 18.956(7)$ Å, $\beta = 92.47(3)^\circ$, $U = 2945(2)$ Å³, $Z = 4$, $D_c = 1.71$ g cm⁻³, $F(000) = 1480$, space group $P2_1/c$ (no. 14); Mo-K α X-radiation ($\lambda = 0.71073$ Å, graphite monochromator), $\mu(\text{Mo-K}\alpha) = 1.25$ mm⁻¹.

The structure was solved, and all non-hydrogen atoms located, by conventional heavy-atom and difference Fourier methods. Phenyl hydrogen atoms were included in calculated positions (C–H 0.96 Å) with fixed isotropic thermal parameters ($U = 8 \times 10^4$ Å²). All non-hydrogen atoms were refined anisotropically, the refinement converging at $R = 0.036$ ($R' = 0.036$) with a weighting scheme of the form $w^{-1} = [\sigma^2(F) + 0.00475|F|^2]$. The only residual electron-density peaks on the final difference synthesis were between -0.51 and 0.40 e Å⁻³. Scattering factors and corrections for anomalous dispersion were taken from ref. 7. All calculations were carried out using a DEC micro-Vax II computer with the SHELXTL PLUS suite of programs.⁸ Selected bond lengths and angles and atomic coordinates are given in Tables 1 and 2 respectively.

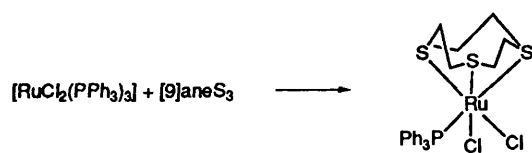
Structure Determination of [RuCl(PPh₃)₃][14]aneS₄]ClO₄.—Yellow prisms were grown as yellow hexagonal plates by diffusion of ethanol into a dichloromethane solution of the crude salt. That chosen for data collection (ca. 0.34 × 0.31 × 0.26 mm) was mounted on a glass fibre. Diffracted intensities were collected (ω–2θ scans) at 301 K on an Enraf-Nonius CAD4 four-circle diffractometer. Of 7303 unique reflections, 6206 had

$I \geq 3\sigma(I)$, and only these data were used in the solution and refinement of the structure. Corrections were applied for Lorentz, polarization and X-ray absorption effects, the latter by analysis of azimuthal ψ -scan data (transmission coefficients 0.9998–0.8835).

Crystal data. $C_{28}H_{35}Cl_2O_4PRuS_4$, $M = 735.82$, monoclinic, $a = 9.245(2)$, $b = 3.885(5)$, $c = 24.305(13)$ Å, $\beta = 95.77(1)^\circ$, $U = 3103.9(13)$ Å³, $D_c = 1.575$ g cm⁻³, $Z = 4$, $F(000) = 1568$, space group $P2_1/n$ (no. 14, alternative setting), Mo-K α X-radiation ($\lambda = 0.71069$ Å, graphite monochromator), $\mu(\text{Mo-K}\alpha) = 0.957$ mm⁻¹.

The structure was solved, and all non-hydrogen atoms located, by conventional direct and difference Fourier methods. All non-hydrogen atoms were refined anisotropically and hydrogen atoms were included in calculated positions. The refinement converged at $R = 0.071$ ($R' = 0.078$) with a weighting scheme of the form $w^{-1} = [\sigma^2(F) + 0.00032|F|^2]$. Scattering factors and corrections for anomalous dispersion were taken from ref. 7. All calculations were carried out as for $[\text{RuCl}_2(\text{PPh}_3)([9]\text{janeS}_3)] \cdot \text{CDCl}_3$. Selected bond lengths and angles and atomic coordinates are given in Tables 3 and 4 respectively.

Additional material available from the Cambridge Crystallographic Data Centre comprises H-atom coordinates, thermal parameters and remaining bond lengths and angles.



Scheme 3

Table 3 Selected bond lengths (Å) and angles (°) for $[\text{RuCl}(\text{PPh}_3)([14]\text{janeS}_4)]^+$ with e.s.d.s in parentheses

Ru–Cl	2.425(1)	Ru–P	2.356(1)
Ru–S(1)	2.286(2)	Ru–S(2)	2.344(2)
Ru–S(3)	2.383(2)	Ru–S(4)	2.359(2)
P–Ru–Cl	91.5(1)	S(1)–Ru–P	90.0(1)
S(2)–Ru–Cl	91.4(1)	S(2)–Ru–P	89.7(1)
S(2)–Ru–S(1)	86.7(1)	S(3)–Ru–Cl	88.2(1)
S(3)–Ru–S(1)	90.3(1)	S(3)–Ru–S(2)	91.5(1)
S(4)–Ru–Cl	87.6(1)	S(4)–Ru–P	94.3(1)
S(4)–Ru–S(1)	94.2(1)	S(4)–Ru–S(3)	84.5(1)

Table 4 Atomic coordinates for $[\text{RuCl}(\text{PPh}_3)([14]\text{janeS}_4)]\text{ClO}_4$

Atom	x	y	z	Atom	x	y	z
Ru	0.101 19(4)	0.207 84(3)	0.098 86(2)	C(9)	-0.219 1(12)	0.260 2(8)	0.170 4(7)
Cl(1)	0.151 25(19)	0.130 15(12)	0.013 46(6)	C(10)	-0.112 9(13)	0.342 3(8)	0.178 4(6)
Cl(2)	0.908 9(2)	0.079 80(12)	0.383 09(8)	C(11)	0.320 3(6)	-0.008 8(4)	0.121 5(2)
S(1)	0.059 3(3)	0.286 76(15)	0.178 26(7)	C(12)	0.416 2(6)	0.022 8(4)	0.085 4(2)
S(2)	0.331 43(17)	0.280 10(11)	0.108 21(7)	C(13)	0.519 2(7)	-0.041 2(5)	0.067 0(3)
S(3)	0.000 4(3)	0.339 55(14)	0.045 01(8)	C(14)	0.521 4(8)	-0.134 3(5)	0.084 0(3)
S(4)	-0.135 71(18)	0.143 50(13)	0.084 46(9)	C(15)	0.426 8(8)	-0.166 9(5)	0.120 7(3)
P	0.196 13(15)	0.075 74(9)	0.151 60(5)	C(16)	0.328 6(7)	-0.103 3(5)	0.140 3(3)
O(1)	0.812 8(8)	0.147 2(5)	0.400 2(3)	C(21)	0.053 7(6)	-0.005 3(4)	0.169 7(2)
O(2)	0.850 7(8)	-0.015 1(5)	0.382 7(4)	C(22)	-0.010 4(6)	-0.063 9(4)	0.125 9(2)
O(3)	1.037 2(9)	0.085 1(5)	0.416 7(5)	C(23)	-0.121 3(7)	-0.126 0(5)	0.134 2(3)
O(4)	0.934 4(14)	0.105 0(8)	0.329 2(4)	C(24)	-0.179 5(7)	-0.127 5(5)	0.185 1(3)
C(1)	0.180 4(11)	0.398 2(6)	0.175 7(5)	C(25)	-0.119 8(8)	-0.068 6(6)	0.227 2(3)
C(2)	0.326 0(10)	0.373 3(6)	0.162 3(3)	C(26)	-0.004 6(7)	-0.008 7(4)	0.219 3(3)
C(3)	0.356 9(8)	0.350 3(5)	0.047 8(3)	C(31)	0.308 7(6)	0.104 3(4)	0.217 4(2)
C(4)	0.239 3(10)	0.419 8(6)	0.025 1(4)	C(32)	0.458 3(7)	0.089 1(5)	0.221 6(3)
C(5)	0.111 0(13)	0.376 1(8)	-0.005 3(5)	C(33)	0.546 2(8)	0.109 3(5)	0.270 3(3)
C(6)	-0.158 8(18)	0.280 3(8)	-0.003 1(5)	C(34)	0.484 1(9)	0.144 6(5)	0.315 0(3)
C(7)	-0.208 7(13)	0.178 6(8)	0.015 1(5)	C(35)	0.338 0(9)	0.160 4(5)	0.311 7(3)
C(8)	-0.251 3(12)	0.202 8(13)	0.125 9(7)	C(36)	0.251 5(8)	0.142 6(4)	0.263 2(3)

Results and Discussion

The complex $[\text{RuCl}_2(\text{PPh}_3)_3]$ reacts slowly with $[9]\text{janeS}_3$ in dichloromethane under ambient conditions to provide a yellow compound formulated as $[\text{RuCl}_2(\text{PPh}_3)([9]\text{janeS}_3)]$ on the basis of spectroscopic data (Scheme 3).

The appearance of two absorptions in the far-IR spectrum suggests a *cis*- RuCl_2 unit and the appearance of one resonance at δ 35.0 in the ³¹P NMR spectrum indicates only one phosphine environment. Integration of the ¹H NMR spectrum indicates that the phosphine and $[9]\text{janeS}_3$ are present in a 1:1 ratio. Given the propensity of the $[9]\text{janeS}_3$ ligand to act as a tridentate facial ligand and not withstanding the possibility of endodentate co-ordination¹ with reduced denticity, a simple 'piano-stool' arrangement appeared likely rather than a polynuclear species, despite the low solubility of the complex.

During this study the reaction between $[\text{RuCl}_2(\text{PPh}_3)_3]$ and $[9]\text{janeS}_3$ was referred to in a review,² which supported our formulation for $[\text{RuCl}_2(\text{PPh}_3)([9]\text{janeS}_3)]$; however we wished to establish firmly the co-ordination geometry. The formulation was therefore confirmed by a single-crystal X-ray diffraction analysis and the pseudooctahedral mononuclear nature of

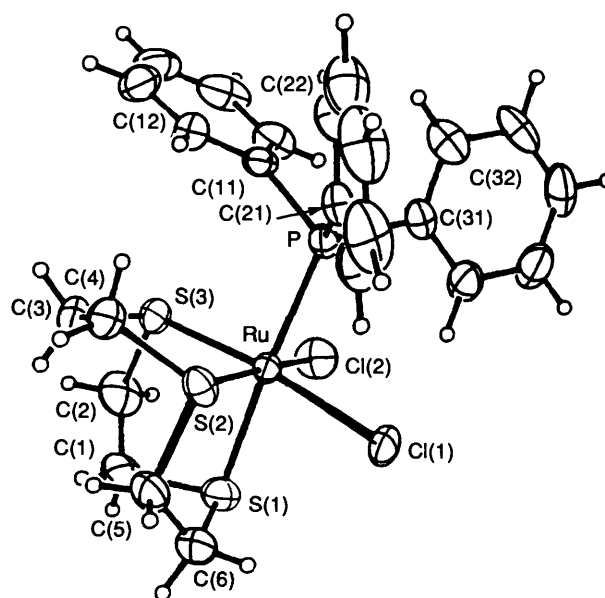


Fig. 1 Molecular geometry of $[\text{RuCl}_2(\text{PPh}_3)([9]\text{janeS}_3)] \cdot \text{CDCl}_3$

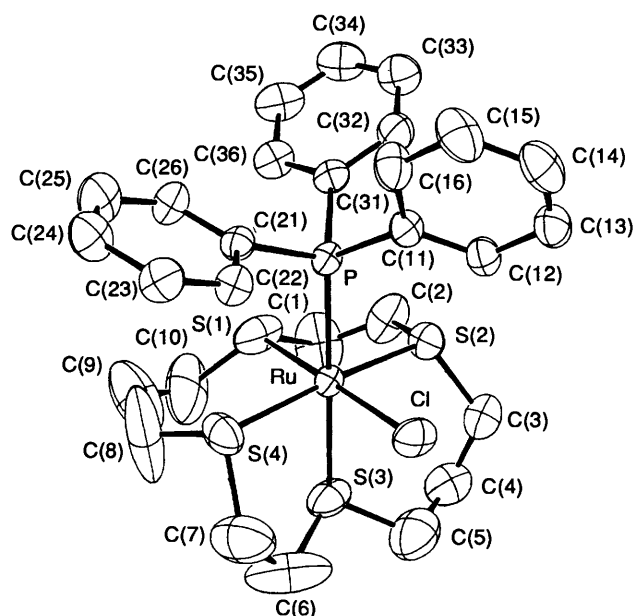


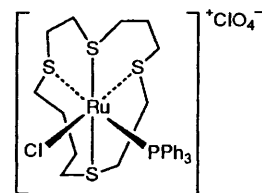
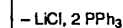
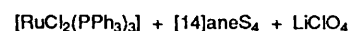
Fig. 2 Molecular geometry of $[\text{RuCl}(\text{PPh}_3)([\text{14}] \text{aneS}_4)]^+$. Hydrogen atoms are omitted for clarity

the complex established (Fig. 1). The structural parameters associated with the ruthenium co-ordination sphere are close to octahedral despite the comparatively large cone angle of the phosphine ligand. The differential *trans* influence of the phosphine and chloride ligands may be inferred from the relative Ru–S bond lengths for S(1), S(2) and S(3) from which it is apparent that the longest Ru–S interaction occurs for the sulfur *trans* to the phosphine ligand even though the steric bulk of the PPh_3 ligand would be expected to favour a lengthening of the Ru–S(2) and Ru–S(3) bonds. Whilst this might be accommodated by a simple σ -*trans* influence argument it is also interesting to consider the possibility that competitive π acceptance plays a role in the destabilisation of the Ru–S(1) interaction.

The compound has a surprisingly low solubility in common organic solvents and this may be due in part to an extensive hydrogen-bonding network which is built up in the crystal by interaction of the chlorine atoms of the solvent of crystallization (deuteriochloroform) and the protons bound to the metallocycle. The co-ordination of sulfur macrocycles to metals appears to enhance the acidity of C–H bonds α to sulfur and we anticipate this feature will become increasingly important as the reactivity of this class of compounds comes under study, although this property may ultimately compromise the anticipated application of thia crown ethers to catalyst design.

Whilst a similar reaction ensued with $[\text{RuCl}_2(\text{PPh}_3)_3]$ and $[\text{14}] \text{aneS}_4$, a chloride salt was obtained rather than a neutral complex as observed with $[\text{9}] \text{aneS}_3$ (Scheme 4). More crystalline samples were obtained by metathesis of the chloride for either AsF_6^- or ClO_4^- , the latter providing single crystals suitable for X-ray diffractometry.

The spectroscopic data suggested the formulation $[\text{RuCl}(\text{PPh}_3)([\text{14}] \text{aneS}_4)]^+$. In addition to a molecular ion being observed in the FAB mass spectrum, ^1H NMR integration indicated a macrocycle to phosphine ratio of 1 : 1 whilst the far-IR spectrum showed only one absorption attributable to $\nu(\text{RuCl})$ at 275 cm^{-1} . The co-ordination geometry (*cis* or *trans*) could not be determined unequivocally by spectroscopic techniques, however a single-crystal X-ray diffraction analysis of the perchlorate salt indicated that a *cis* arrangement of chloride and phosphine ligands is adopted and that the co-ordination geometry at ruthenium is once again essentially



Scheme 4

octahedral (Fig. 2). As with the neutral complex $[\text{RuCl}_2(\text{PPh}_3)([\text{9}] \text{aneS}_3)]$, a differential *trans* influence between the phosphine and chloride ligands is apparent such that the Ru–S interaction *trans* to the phosphine is the longest and that *trans* to the chloride the shortest.

The adoption of a *cis* disposition for the chloride and phosphine ligands would appear to be consistent with a stepwise chelation of the four sulfur donor atoms following successive extrusion of ligands at the ruthenium centre. It is believed that the small size of the ring of $[\text{14}] \text{aneS}_4$ disfavours the adoption of the *trans* geometry in octahedral complexes¹ and this has been clearly illustrated for the complexes *cis*- $[\text{RhCl}_2([\text{14}] \text{aneS}_4)]^+$ and *trans*- $[\text{RhCl}_2([\text{16}] \text{aneS}_4)]^+$ ($[\text{16}] \text{aneS}_4 = 1,5,9,13$ -tetrathiacyclohexadecane).⁹ An example of the *trans* arrangement of co-ligands has however been obtained for a ruthenium complex of permethylated $[\text{14}] \text{aneS}_4$. Thus the conversion of *cis*- $[\text{RuCl}_2(\text{Me}_4[\text{14}] \text{aneS}_4)]^+$ to *trans*- $[\text{RuCl}(\text{Me}_4[\text{14}] \text{aneS}_4)]^+$ ($\text{Me}_4[\text{14}] \text{aneS}_4 = 6,6,13,13$ -tetramethyl-1,4,8,11-tetrathiacyclohexadecane)¹⁰ is accompanied by a change in geometry which is counter-intuitive if only the steric requirements of the two co-ligands are considered. In this case the added steric congestion introduced by permethylation presumably disfavours the accumulation of sulfur donors on two mutually perpendicular meridional planes. The dinuclear pseudo-square-planar complex $[\{\text{Rh}(\text{Me}_4[\text{14}] \text{aneS}_4)\}_2]^{2+}$ also features a *trans* arrangement of the sulfur macrocycle,¹¹ however this is presumably due to the requirement of a square-planar geometry for four-co-ordinate d^8 rhodium.

The wide range of conveniently available labile poly-(triphenylphosphine) complexes of the platinum group metals suggests many precursors suitable for the introduction of thia crown ethers into co-ordination spheres with diverse ligand sets and reactivities, a possibility which we are currently investigating.

Following the submission of this paper the reaction of $[\text{RuCl}_2(\text{PPh}_3)_3]$ with 1,4,7,10,13-pentathiacyclopentadecane ($[\text{15}] \text{aneS}_3$) and sodium tetraphenylborate has been described and the product, $[\text{Ru}(\text{PPh}_3)([\text{15}] \text{aneS}_3)]\text{BPh}_4$, crystallographically characterized.¹²

Acknowledgements

We thank Johnson Matthey Chemicals for a generous loan of ruthenium salts. We are grateful to Dr. M. Schröder for helpful discussions and communicating unpublished results. A. F. H. thanks Professor W. R. Roper and the University of Auckland, Department of Chemistry, for the generous provision of research facilities.

References

- 1 S. Cooper and S. C. Rawle, *Struct. Bonding (Berlin)*, 1990, **72**, 1.
- 2 (a) A. J. Blake and M. Schröder, *Adv. Inorg. Chem.*, 1990, **35**, 1; (b) R. M. Christie, Ph.D. Thesis, University of Edinburgh, 1989.
- 3 A. J. Blake, M. A. Halcrow and M. Schröder, *J. Chem. Soc., Chem. Commun.*, 1991, 253.

- 4 J. C. Cannadine, A. L. Hector and A. F. Hill, *Organometallics*, 1992, **11**, 2323.
- 5 A. F. Hill, N. W. Alcock, J. C. Cannadine and G. R. Clark, *J. Organomet. Chem.*, 1992, **426**, C40.
- 6 J. A. Osborn, F. H. Hardin, F. J. Young and G. Wilkinson, *J. Chem. Soc.*, 1966, 1711.
- 7 *International Tables for X-Ray Crystallography*, Kynoch Press, Birmingham, 1974, vol. 4.
- 8 G. M. Sheldrick, SHELXTL-PLUS programs for use with the Nicolet X-ray system, Revision 4.0, Göttingen, 1990.
- 9 A. J. Blake, G. Reid and M. Schröder, *J. Chem. Soc., Dalton Trans.*, 1989, 1675.
- 10 T. Yoshida, T. Adachi, T. Ueda, T. Tanaka and F. Goto, *J. Chem. Soc., Chem. Commun.*, 1990, 342.
- 11 T. Yoshida, T. Ueda, T. Adachi, K. Yamamoto and T. Higuchi, *J. Chem. Soc., Chem. Commun.*, 1985, 1137.
- 12 A. J. Blake, G. Reid and M. Schröder, *Polyhedron*, 1992, **11**, 2501.

Received 4th September 1992; Paper 2/04773J